Finite-element analysis of SHPB tests on double-lap adhesive joints

Georges Challita, Ramzi Othman

Finite-element analysis of SHPB tests on double-lap adhesive joints

Georges Challita [a,b], Ramzi Othman [a]

[a] Institut de Recherche en Génie Civil et Mécanique, Ecole Centrale de Nantes, 1 Rue de la Noë BP 92101, 44321 Nantes cedex 3, France
[b] Département de Mécanique, Faculté de Génie Branche 2, Université Libanaise, Beyrouth, Lebanon

Adhesively bonded assemblies are in increasing use in multiple engineering applications. However, they can endure impact loads. The measurement, of these assemblies mechanical behaviour, under dynamic loads is of great concern. Several works used the split Hopkinson pressure bar (SHPB) method to assess the strength of adhesive joints at high loading rates. In this paper, we investigated the accuracy of SHPB tests on double-lap bonded joints by three-dimensional finite-element analysis. For this analysis, an elastic behaviour is assumed for both adherends and adhesive. We were interested in the influence of material, geometrical and dynamic parameters on the SHPB accuracy. From this study, we can conclude that the SHPB bar method gives a good estimation of the mean adhesive stress value. However, its estimation, to the mean adhesive strain and to the maximum adhesive stress and strain, is rather bad. A unified parameter is therefore proposed to help designing specimens and to correct the SHPB results.

Keywords:
M. Lap-shear
M. Stress distribution
P. Impact
Finite-element
Hopkinson bar

1. Introduction

The interest in bonded assemblies is in a continuous increase in recent years. This is partly due to lightening and cost effectiveness. Furthermore, adhesives can be used to bond together parts of structures that cannot be welded. This is the case of dissimilar materials bonding. Many works were carried out to understand and measure the strength of these joints under quasi-static loads. Nevertheless, these joints may endure impact loads as they are used for example in automobile and aircraft structures. Less works were interested in the mechanical behaviour of bonded joints submitted to impact loads. These works investigated the impact response from an experimental [1–21] and numerical [22–30] point of view. They were interested either in the adhesive strength [2–20] or the stress distribution and wave propagation in the joint [21,23–30].

The majority of experimental works were focused on the measurement of the impact strength of adhesive joints. Several kinds of loads were investigated, mainly tensile [4–7] and shear [8–18]. Furthermore, some works interested in the strength of electronic packages [19,20]. However, a variety of techniques and sample shapes can be found in literature. This is due to the lack of standards. Indeed, there are two standards for the dynamic mechanical testing of adhesively bonded joints: the ASTM D950-03 [31] and ISO EN 11343 adhesives [32]. The first standard deals with pendulum impact test whereas the second interests in the wedge impact test. Unfortunately, these two tests have a major problem: they can only give comparative results which are not suitable for design. Furthermore, these standards do not deal with the most used set-up: the split Hopkinson pressure bar (SHPB) [12–17]. This set-up is the most accurate device for testing the dynamic behaviour of materials at high strain rates. Its main asset is the simple and accurate modelling of the wave propagation. Indeed, this set-up is mainly made-up of two (visco)-elastic bars. A one-dimensional wave propagation model, which takes into consideration wave dispersion, gives highly good estimation. This set-up was first used for adhesively bonded joints in Ref. [12]. Subsequently, this work was followed by Refs. [13–17]. Recently, the SHPB set-up has become more interesting as it was extended to intermediate strain-rate range [33,34] by applying a redundant-measurement wave separation technique [35,36]. This means that SHPB set-up can be used, for example, to measure the adhesive joint strength at impact velocities ranging from 0.1 to 30 m/s; which is a very wide and promising range of impact velocities. However, there is no standard for this method.

In a SHPB set-up a strain gauge station is cemented on each bar. The strain and the stress inside the specimen are recovered from the analysis of the two gauge signals. However, this analysis assumes that the strain and the stress fields are homogenous in the tested sample, i.e., that a dynamic equilibrium state is reached in the specimen for the most of the test duration. This assumption allows recovering an estimation of the mean values of the stress and the strain fields. However, the equilibrium state is reached belatedly when testing soft materials or when tests are carried

out at very high strain rates (or impact velocities). If the time, during which the tested sample is deformed heterogeneously, becomes significant compared to the whole tested duration, the conventional theory of the SHPB technique will be no more valid and other solutions are needed [38–42]. The problem of heterogeneity of the strain and stress fields is not intrinsic to the SHPB set-up. It can be found for all dynamic facilities wherever low strength materials are considered. The dynamic-induced heterogeneity is influenced by the loading rise time and the wave propagation time to go through the specimen. Therefore, pulse load shaping induces faster dynamic equilibrium achievement [16,43,44]. However, the material behaviour should be known beforehand to design the pulse shaper.

In addition to the dynamic-induced heterogeneity of the strain and the stress fields discussed in the above paragraph, the adhesive joint sample suffers heterogeneous stress and strain distribution even in quasi-static tests. Indeed, there is a peak of stress and strain near the joint edges whereas the two fields are quasi-homogeneous elsewhere. This phenomenon was widely investigated when joints are submitted to quasi-static loads (see for example Refs. [45–47]).

Consequently, the heterogeneity of the stress or strain field in adhesively bonded samples has two onsets: (i) the structural effects of joints, which occur even under quasi-static conditions; and (ii) the dynamic-induced heterogeneity which is originated by the finite waves speeds. Both effects are a priori coupled. Therefore, the stress distribution should be studied under dynamic conditions.

Some works were interested in the stress distribution in the case of impact loads. Zachary and Burger [21] studied the wave propagation through a single-lap joint by photo-elasticity. The other works analysed the problem by finite element method to investigate the bending [24–26], tensile [27] and shear [28–30] impacts. However, all the above cited works only interested in the stress distribution. The strain distribution was not considered. Furthermore, they did not correlate the stress distribution with the accuracy of an experimental set-up to estimate the joint's strength. These works conclusions are helpful for engineering design. However, they are insufficient to estimate the accuracy of the dynamic facilities when measuring the strength of adhesive joints. Only, Adams and Harris [23] investigated the accuracy of the impact method by finite element analysis. However, they only investigated impact angles effects with a quasi-static numerical model.

Therefore, this paper aims at quantifying the accuracy of the shear stress and strain measurements by the SHPB technique. The double-lap joint is considered here as it reduces peel effects. The analysis is carried out by commercial finite element software (ABAQUS 6.6-2). Precisely, we study in this work the sensitivity of the SHPB accuracy to several parameters. We are interested in both stress and strain measurements. This study is limited to the case of an elastic behaviour of the adhesive and adherends.

2. Method

2.1. Brief recall of the SHPB method

As we are interested in the accuracy of the SHPB, we will briefly introduce this technique below. For an extended review of this method, the reader is referred to Refs. [48–51].

The conventional configuration (Fig. 1) is due to Kolsky [52] and was inspired from the work of Hopkinson [53]. This configuration is dedicated to the compression testing. The SHPB system is made of two elastic bars. Both have usually the same diameter and are made of the same material. The tested sample is

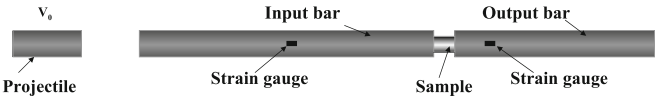

Fig. 1. Schematic of a SHPB set-up.

sandwiched between the two bars. The load is generated by the impact of a projectile on the first bar, also called the input bar. The projectile has usually the same diameter and material as the main two bars. The impact of the projectile generates an incident compressive wave, ε_{inc}, in the input bar. This wave propagates till the specimen–input bar interface. A part of this wave is reflected back as a tensile wave: ε_{ref}. A second part is transmitted, through the specimen, to the second bar as a transmitted compressive wave ε_{tra}. The second bar is also called the output bar.

On each bar a strain gauge station is cemented. The length of the projectile is chosen to be short enough to separate incident and reflected waves. On the other hand, the output bar strain gauge measures directly the transmitted wave. However, the three waves are actually measured long away from the tested sample. Therefore, they should be shifted to the sample–bars interfaces knowing the bars' wave dispersion relations [54,55].

By assuming (i) one-dimensional stress-state and (ii) homogeneous stress and strain fields in the specimen, the mean nominal stress and longitudinal strain rate, in the specimen, are given by

$$\sigma(t) = E_b A_b \frac{\varepsilon_{inc}(t) + \varepsilon_{ref}(t) + \varepsilon_{tra}(t)}{2A_s}, \tag{1}$$

and

$$\dot{\varepsilon}_l(t) = c_0 \frac{\varepsilon_{inc}(t) - \varepsilon_{ref}(t) - \varepsilon_{tra}(t)}{l_s}, \tag{2}$$

respectively. In Eqs. (1) and (2), it E_b holds for the bars Young's modulus, A_b and A_s hold for the bar and the sample cross-sectional area, respectively, and c_0 holds for the sound speed in the bar. The nominal mean strain in the specimen is given by

$$\varepsilon_l(t) = \int_0^t \dot{\varepsilon}_l(\tau)\, d\tau. \tag{3}$$

The behaviour of the tested material is therefore recovered from the incident, reflected and transmitted waves by Eqs. (1)–(3).

2.2. Sample geometry

In the SHPB configuration presented above, the compressive behaviour is considered. However, we are interested here in the shear behaviour of the adhesively bonded joints. In this paper we propose a double-lap bonded joint [17]. Indeed, peel stress, with this geometry, is less important than in a single-lap joint [16].

The adopted geometry, in this paper, is presented in Fig. 2. The adherends are three plates. The central adherend is shifted horizontally to induce the shear stress. The lower and the upper adherends have the same geometry and are made of the same material. The adhesive layers are also assumed to be similar. Below, the subscripts 0 and 1 hold for the adhesive layers and the central adherend, respectively; whereas, the subscript 2 holds for the lower and upper adherends.

The sample is sandwiched between the input and output bars as presented in Fig. 3. The compressive load is transformed, due to the sample geometry, to a shear stress in the adhesive joints. To recover the stress and the strain in the adhesive layer, we

- consider the same assumption as in the conventional configuration;

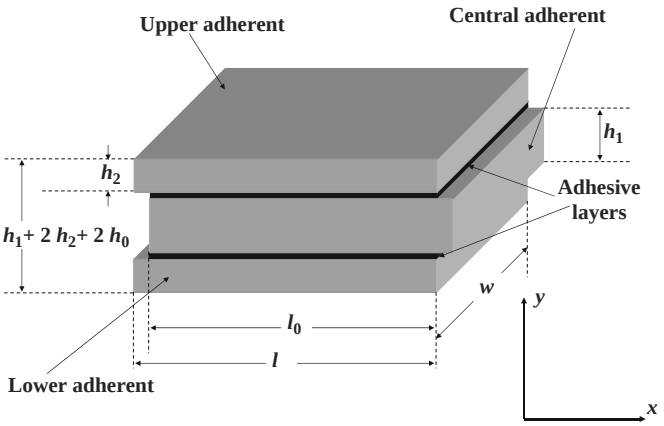

Fig. 2. Sample geometry.

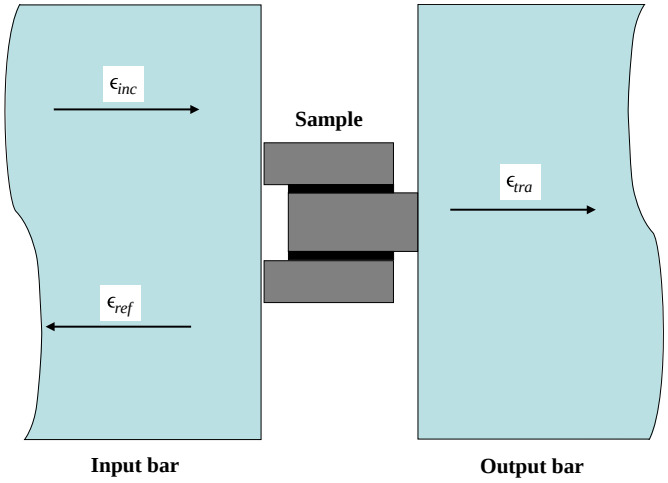

Fig. 3. New sample sandwiched between the two bars.

- assume that the adherends are sufficiently stiff and remain non-deformed during the test.

Therefore, the shear stress, strain rate and strain in the adhesive layer are written as follows:

$$\sigma_{xy}(t) = E_b A_b \frac{\varepsilon_{inc}(t)+\varepsilon_{ref}(t)+\varepsilon_{tra}(t)}{4 l_0 w}, \tag{4}$$

$$\dot{\varepsilon}_{xy}(t) = c_0 \frac{\varepsilon_{inc}(t)-\varepsilon_{ref}(t)-\varepsilon_{tra}(t)}{h_0}, \tag{5}$$

and

$$\varepsilon_{xy}(t) = \int_0^t \dot{\varepsilon}_{xy}(\tau)\, d\tau, \tag{6}$$

respectively. In Eqs. (4)–(6), l_0, w, h_0 hold for the overlap length, sample width and adhesive thickness, respectively.

2.3. Numerical model

In order to measure the accuracy of the SHPB method while testing a double-lap bonded joint, we developed a numerical model of the whole set-up on commercial finite element software (ABAQUS 6.6-2). The explicit integration module is used. In this model, we considered the two bars and the sample. On the left side of the input bar, we impose a velocity step as shown in Fig. 5. τ_r and τ_d are the rise- and drop-time, respectively. In addition, we fix the right side of the output bar. The specimen–bars interfaces are supposed frictionless. The bars, adherends and adhesive are assumed to have an elastic behaviour. E_b, E_0, E_1 and E_2 are Young's modulii of the bars, adhesive, central adherend and lower adherend, respectively. The upper adherend has the same properties as the lower. Due to symmetry reasons, only a quarter of the set-up is modelled. The bars, adherends and adhesive layers are meshed with 8-node three-dimensional linear elements. An example of the used mesh is presented in Fig. 4.

Each simulation is carried out during 0.5 ms. Outputs are stored at a step time of 1 μs. From the all possible outputs we are interested in the following ones:

- the stress and strain fields in adhesive layer, and
- the longitudinal strains at two virtual gauge stations.

2.4. Stress measurement

In order to check the SHPB method accuracy, we define multiple parameters to quantify the method error. In this subsection, we are interested in the measurement of the mean value of the stress field. With a numerical simulation, we reproduce a SHPB test. Hence, we analyse the longitudinal strains simulated at the virtual gauge stations, as they would be obtained

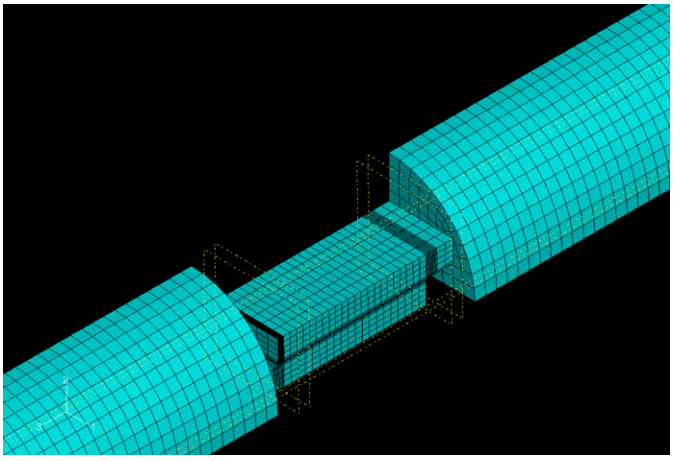

Fig. 4. A mesh example.

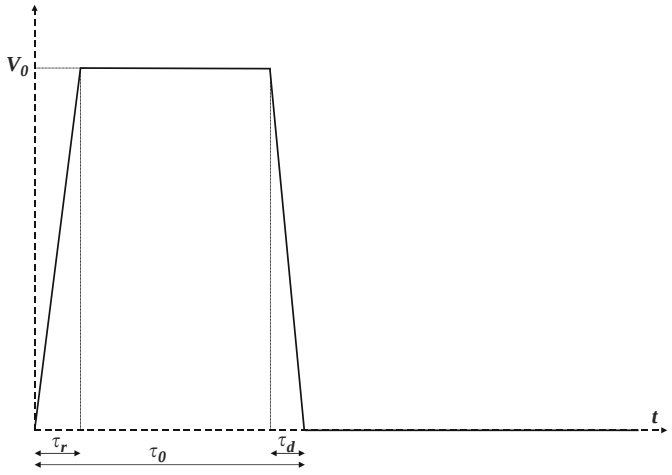

Fig. 5. Imposed velocity at the input bar left side.

in a real experimental test. Indeed, the signal obtained on the input bar gauge is cut into incident and reflected waves. The output bar gauge gives the transmitted wave. Then the three waves are shifted to the specimen–bars interfaces. Note that wave shifting is based on wave dispersion relation which is computed by Zhao and Gary method [54].

Once the three waves are shifted, the shear stress in the adhesive, as measured by a SHPB set-up, is given by (Eq. (4))

$$\sigma_{xy}^{SHPB}(t) = E_b A_b \frac{\varepsilon_{inc}(t)+\varepsilon_{ref}(t)+\varepsilon_{tra}(t)}{4 l_0 w}. \tag{7}$$

σ_{xy}^{SHPB} is an approximation of the mean value of the shear stress σ_{xy}^{avg} which can be written as

$$\sigma_{xy}^{avg}(t) \equiv \frac{1}{l_0 h_0 w}\int_0^{l_0}\int_0^{h_0}\int_0^{w} \sigma_{xy}(x,y,z,t)\,dx\,dy\,dz, \tag{8}$$

where $\sigma_{xy}(x,y,z,t)$ is the shear stress field in the adhesive layer.

In order to quantify the error of the SHPB method, we measure the ratio of the mean stress in the adhesive layer (Eq. (7)) to the stress given by the SHPB method (Eq. (8)):

$$\beta_\sigma(t) \equiv \frac{\sigma_{xy}^{avg}(t)}{\sigma_{xy}^{SHPB}(t)}. \tag{9}$$

Obviously, the SHPB has a good accuracy if this ratio is almost equal to 1.

2.5. Strain measurement

The same work carried in Section 2.4 with the shear stress, can be carried here with the shear strain. Indeed, by applying the SHPB analysis to the three waves: incident, reflected and transmitted, we can recover the shear strain, as measured by a SHPB set-up (Eqs. (5)–(6)):

$$\varepsilon_{xy}^{SHPB}(t) = \int_0^t c_0 \frac{\varepsilon_{inc}(\tau)-\varepsilon_{ref}(\tau)-\varepsilon_{tra}(\tau)}{h_0} d\tau. \tag{10}$$

$\varepsilon_{xy}^{SHPB}(t)$ should be an approximation of the mean shear strain value, $\varepsilon_{xy}^{avg}(t)$. This mean value can be expressed as

$$\varepsilon_{xy}^{avg}(t) \equiv \frac{1}{l_0 h_0 w}\int_0^{l_0}\int_0^{h_0}\int_0^{w} \varepsilon_{xy}(x,y,z,t)\,dx\,dy\,dz, \tag{11}$$

where $\varepsilon_{xy}(x,y,z,t)$ is the shear strain field in the adhesive layer. Similar to Eq. (9), we define $\beta_\varepsilon(t)$ as the ratio between strains given by Eqs. (10) and (11)

$$\beta_\varepsilon(t) \equiv \frac{\sigma_{xy}^{avg}(t)}{\sigma_{xy}^{SHPB}(t)}. \tag{12}$$

2.6. Homogeneity of stress field

Firstly, we recall that one of this paper's aims is to study the homogeneity of the stress and strain. Similar to Meng and Li [37] and Aloui et al. [42] the homogeneity of the stress field will be measured by the following coefficient:

$$\alpha_\sigma(t) \equiv \sqrt{\frac{1}{l_0 h_0 w}\int_0^{l_0}\int_0^{h_0}\int_0^{w} \frac{|\sigma_{xy}(x,y,z,t)|^2-|\sigma_{xy}^{avg}(t)|^2}{|\sigma_{xy}^{avg}(t)|^2}\,dx\,dy\,dz}. \tag{13}$$

This coefficient measures the homogeneity of the stress field in the adhesive layer. When this coefficient is insignificant $\alpha_\sigma \ll 1$, the stress field is quasi-homogeneous. In this case, the stress field can be approximated by its mean value $\sigma_{xy}^{avg}(t)$ [37,42].

On the other hand, the homogeneity of the stress field can also be measured by the ratio of the maximum to the mean value, i.e.,

$$\chi_\sigma(t) \equiv \frac{\sigma_{xy}^{avg}(t)}{\max_x\left[\frac{1}{h_0 w}\int_0^{h_0}\int_0^{w} \sigma_{xy}(x,y,z,t)\,dy\,dz\right]}. \tag{14}$$

2.7. Homogeneity of strain field

In order to measure the homogeneity of the strain field, we define homogeneity coefficients similar to those defined to measure the homogeneity of the stress field. Precisely, we consider the α_ε and χ_ε which are defined by

$$\alpha_\varepsilon(t) \equiv \sqrt{\frac{1}{l_0 h_0 w}\int_0^{l_0}\int_0^{h_0}\int_0^{w} \frac{|\varepsilon_{xy}(x,y,z,t)|^2-|\varepsilon_{xy}^{avg}(t)|^2}{|\varepsilon_{xy}^{avg}(t)|^2}\,dx\,dy\,dz}. \tag{15}$$

$$\chi_\varepsilon(t) \equiv \frac{\varepsilon_{xy}^{avg}(t)}{\max_x\left[\frac{1}{h_0 w}\int_0^{h_0}\int_0^{w} \varepsilon_{xy}(x,y,z,t)\,dy\,dz\right]}. \tag{16}$$

It is worth to notice that χ_σ and χ_ε ratios can be used to recover the maximum stress and strain in the joint from the mean stress and strain, respectively.

2.8. Pure-shear assumption

In a single-lap joint, peel and shear may mix [18]. The measured shear strengths with a single-lap joint is the contribution of these two stresses. Therefore, it is of much importance that to check if the stress in a double-lap joint remains a pure shear. Hence, we define the following coefficient to measure the pure-shear stress assumption:

$$\rho_\sigma(t) \equiv \frac{1}{l_0 h_0 w}\int_0^{l_0}\int_0^{h_0}\int_0^{w} \frac{|\sigma_{yy}(x,y,z,t)|}{|\sigma_{xy}(x,y,z,t)|}\,dx\,dy\,dz. \tag{17}$$

3. Results

3.1. Reference model

In order to investigate the influence of material, geometrical and dynamic parameters, we define a reference model. Subsequently, only one parameter will be changed each time. In the reference model, we consider the parameters given in Tables 1 and 2. Furthermore, the input and output virtual gauges are taken as 500 and 200 mm from the specimen.

In Fig. 6(a), we compare the mean value of the strain in the adhesive layer (Eq. (11)) with the strain recovered by the SHPB method (Eq. (10)). It comes from this plot that the SHPB method can highly overestimate the strain in the adhesive. Indeed, in Eq. (11), it is assumed that adherends are not deformed during the test. This is not true. Precisely, the adherends are submitted to compressive deformation near the bars. Furthermore, they are submitted to shear deformation in the neighbourhood of the adhesive layer. The adhesive mean strain to SHPB-recovered strain ratio, i.e., β_ε, is plotted in Fig. 7(b). This ratio varies at the beginning of the test. After $t_h \approx 17\,\mu s$, β_ε is approximately constant and is about 25%. In Fig. 6(a), we plot also the maximum strain in the adhesive layer. This maximum strain is obtained near the adhesive extremities. The mean to maximum strain ratio (χ_ε) is almost constant after $t_h \approx 17\,\mu s$ (Fig. 7(c)) and the mean value is about 83% of the maximum value.

Similarly, we compare the mean and maximum Abaqus stresses to the SHPB stress in Fig. 6(b). It comes that the SHPB method gives an accurate estimation of the mean value. Therefore, the mean stress to the SHPB stress ratio (β_σ) is almost equal to 1 (Fig. 7(b)). However, the specimen geometry concentrates the

Table 1
Material parameters.

	Young's modulus (GPa)	Poisson's ratio	Density (kg/m^3)
Adhesive	1	0.4	1200
Adherends	200	0.3	7800
Input and output bars	200	0.3	7800

Table 2
Geometrical parameters.

	Length (mm)	Width (mm)	Thickness (mm)	Diameter (mm)
Adhesive	14	12	0.1	
Central adherend	16	12	4	
Upper and lower adherends	16	12	4	
Input bar	1000			16
Output bar	600			16

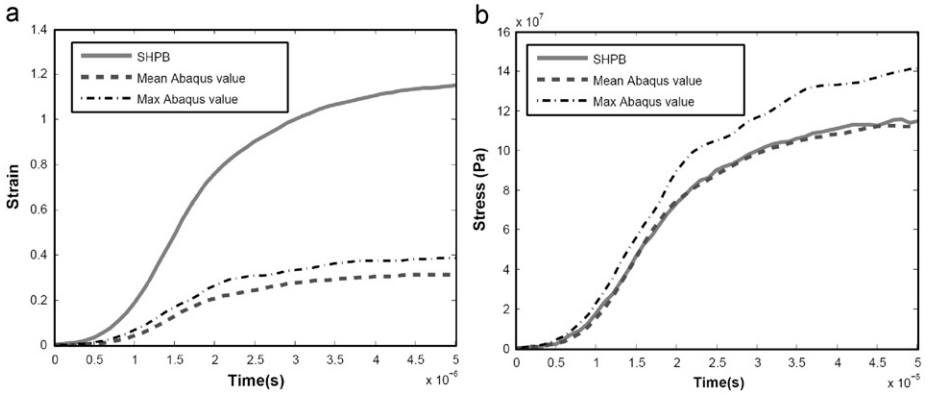

Fig. 6. Comparison between stress and strain recovered by the SHPB method and the maximum and the mean strain and stress values, respectively: (a) strain curves and (b) stress curves.

stress near the adhesive ends. Consequently, the mean to maximum stress ratio (χ_σ) is not equal to 1 (Fig. 7(c)).

α_σ and χ_σ are almost equal to α_ε and χ_ε, respectively. This means that the homogeneity of the stress and strain field have approximately the same behaviour. It is an intuitive result as stress and strain are related with the elastic constants. On the other hand, β_ε and β_σ. These coefficients measure the accuracy of the SHPB to recover the mean stress and strain in the adhesive. The stress in the adhesive is computed from two forces applied at adherends boundaries (Eq. (7)). The SHPB method assumes that the boundary forces are integrally transmitted to the adhesive. This seems to be valid as β_σ is almost equal to 1. To compute the strain, the SHPB method assumes that adherends are rigid and all deformation happen in the adhesive only. Then, the strain is computed from displacements recorded and adherends boundaries (Eq. (10)). As $\beta_\varepsilon < 1$, the adherends seems not to be rigid. That is why the SHPB method overestimates the strain in adhesive.

It is remarkable that the above discussed ratios become almost constant after $t_h \approx 17\,\mu s$. This time can be interpreted by the dynamic homogenisation of stress and strain fields. Indeed, the stress and strain heterogeneity in adhesively bonded specimen is induced by two effects:

- *dynamic heterogeneity* which is due to wave propagation and inertia reasons, and
- *structural heterogeneity* which is rather due to the specimen geometry.

The structural heterogeneity is intrinsic to the geometry. It will be present during the test. The dynamic heterogeneity disappears after some round trips of the waves in the bar. Therefore, the stress and strain homogeneity coefficients, α_σ and α_ε, are important at the beginning of the test (Fig. 7(a)). This means that stress and strain fields are highly heterogeneous. The two coefficients drop continuously till the time $t_h \approx 17\,\mu s$. At this time the dynamic heterogeneity disappears and only the structural heterogeneity remains. After $t_h \approx 17\,\mu s$, the bonded specimen is deformed under an almost quasi-static state. That is why the above discussed ratios are almost constant.

Finally, we compare in Fig. 7(d), the shear and peel stresses. The peel-to-shear-stresses ratio (ρ_σ) is almost 1%. Therefore, we can assume that the adhesive layer is submitted to a pure-shear stress state.

Below only the sensitivity of the steady-state mean values of the above discussed ratios is analysed, i.e., the mean value of these ratios for times $t > t_h$.

3.2. Influence of material parameters

3.2.1. Influence of adhesive Young's modulus

Four values of the adhesive Young's modulus are considered in order to investigate the influence of this parameter. Besides the reference model (E_0=1 GPa), we studied the following cases: E_0=0.5, 3 and 10 GPa. The steady-state mean value of the defined ratios is plotted in Fig. 8(a).

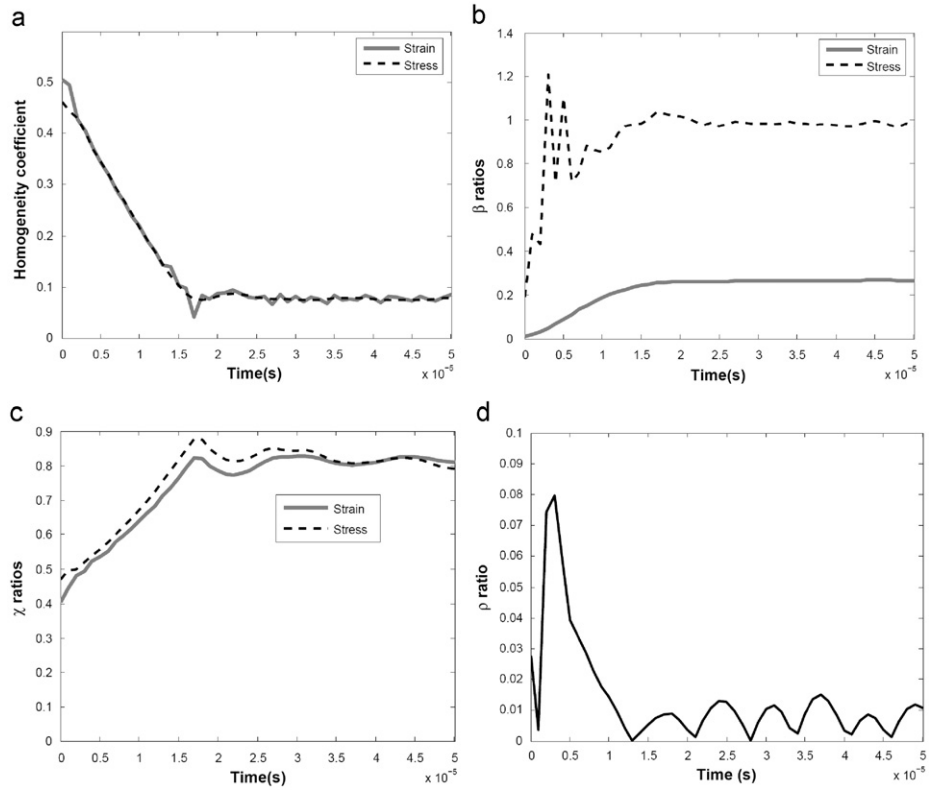

Fig. 7. Variation of the accuracy ratios during the test: (a) homogeneity coefficients, (b) β ratios, (c) χ ratios and (d) ρ ratio.

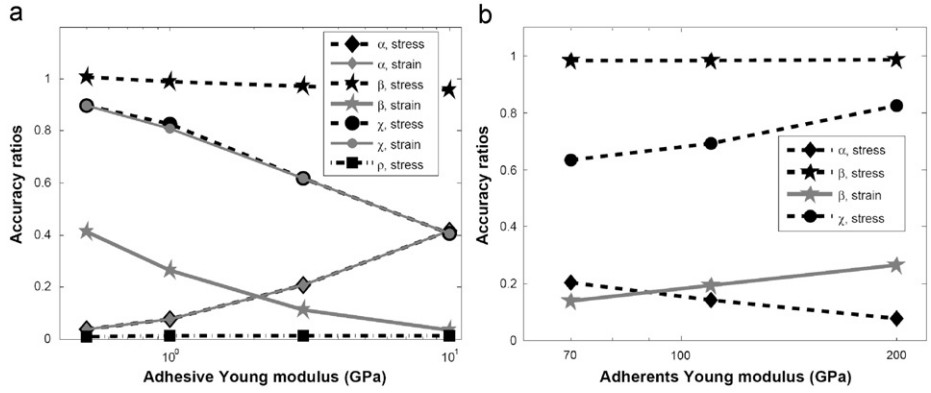

Fig. 8. Influence of material properties: (a) influence of adhesive Young's modulus and (b) influence of adherends Young's modulus.

Firstly, the peel-to-shear-stresses ratio (ρ_σ) is about 1%. For all configurations studied in this paper, ρ_σ remains between 0% and 2%. This ratio will no more be plotted in order to have clearer figures.

Secondly, the stress and strain homogeneity coefficients (α_σ and α_ε, respectively) have almost the same values. They increase when the adhesive Young's modulus increases. The homogeneity of the stress and strain fields is better for low-Young-modulus adhesives. As α_σ and α_ε have almost the same values, only α_σ will be analysed below.

The homogeneity of the stress and strain fields can also be measured by χ_σ and χ_ε, respectively, i.e., the mean-to-maximum ratios. χ_σ and χ_ε decrease when the adhesive Young's modulus increases. This is in line with the conclusions obtained by α ratios as for low Young's modulus values, the stress and strain homogeneity is better. Indeed, for low adhesive Young's modulus values, the situation tends to the case of a deformable adhesive between rigid adherends which yield to constant stress field. Similar to the α ratios, only χ_σ will be analysed below.

Finally, we studied the influence of the adhesive Young's modulus on the β ratios. The β_σ ratio remains almost equal to 1. Therefore, the SHPB method gives a good approximation of the mean stress value. However, β_ε is far lower than 1. The SHPB method overestimates the mean strain values. This point was explained in Section 3.1 yet. β_ε decreases when the adhesive Young's modulus increases. This means that the accuracy on strain measurement of the SHPB method is better for low values of adhesive Young's modulus. In this case, the adherends are much stiffer than the adhesive. The situation tends to the case of deformable adhesive between rigid adherends. Therefore, the adhesive strain can be computed from adherends displacements as assumed by Eq. (10).

It is worth to notice that all ratios are almost linear in terms of the logarithm of the adhesive Young's modulus.

3.2.2. Influence of adherend Young's modulus

Similar to Section 3.2.1, the sensitivities of the defined ratios, to the adherend Young's modulus, are investigated. In all considered configurations, we assumed that the central adherend is made of the same material as the lower and upper adherends. Besides the reference model (E_1 = E_2 = 200 GPa), we studied the following cases: E_1 = E_2 = 70 and 110 GPa. The influence of the adherends Young's modulus is opposite to the adhesive Young's modulus (Fig. 8(b)). Precisely, the increase of the adherends Young's modulus, increases χ_σ, χ_ε and β_ε and decreases α_σ and α_ε. These five ratios are linear-dependent on the logarithm of the adherends Young's modulus. β_σ remains almost constant.

In other words, the stress and strain fields are more homogeneous for high values of adherends Young's modulus. In this situation, the strain measurement by the SHPB method is also more accurate. Indeed, as the adherends Young's modulus increases, the adhesive stiffness becomes insignificant compared to the adherends stiffness. The situation tends to a deformable adhesive between rigid adherends. In this case the stress and strain become constants. Moreover, the adhesive strain can be computed from adherends displacements as assumed by Eq. (10).

3.3. Influence of geometrical parameters

3.3.1. Influence of adhesive thickness

In this section, we analyse three adhesive thicknesses: h_0=50, 100 and 200 μm. The dependence of all ratios on the logarithm of this parameter is almost linear (Fig. 9(a)). Furthermore, χ_σ, χ_ε and β_ε grow while α_σ and α_ε lower when the adhesive thickness increases. However, β_σ remains almost constant.

3.3.2. Influence of adherends thicknesses

In order to investigate the influence of the adherends thicknesses, we consider first that h_1=2h_2, i.e., the central adherend thickness is equal to twice the lower (or upper) adherend thickness. In this case, four values of the central adherend thickness are considered. Precisely, h_1=2, 4, 6 and 8 mm. The dependency of the studied parameters on the central adherend thicknesses has the same tendency as the dependency on the adhesive thickness (Fig. 9(b)). Precisely, we obtain linear dependency on the logarithm of the adherend thickness. Besides, the ratios χ_σ, χ_ε and β_ε are increasing, whereas the ratios α_σ and α_ε are decreasing. Finally, β_σ remains almost constant.

On the other hand, we compared the case where h_1=2h_2= 4 mm (called '242') to the case where h_1=h_2=3 mm (called '333'). The results are plotted in (Fig. 9(c)). It comes from this plot that SHPB method will have the same accuracy in both cases. Indeed, β_σ and β_ε are almost the same. Moreover, the stress and strain fields are more homogeneous in the case of h_1=2h_2 than the case of h_1=h_2. It will be preferable to use the specimen geometry that verifies h_1=2h_2.

3.3.3. Influence of the overlap length

In addition to the influence of the adhesive and adherends thicknesses, we studied the influence of the overlap length. For this purpose, we consider six overlap lengths: l=8, 10, 12, 14, 16 and 18 mm. The results are plotted in Fig. 9(d). The influence of the overlap length is opposite to that of the adhesive and adherends thicknesses.

3.4. Influence of dynamical parameters

3.4.1. Influence of the impact velocity

Generally, the striker impact velocity reached in a conventional SHPB test ranges from 5 to 20 m/s. Therefore, three values of the striker impact velocity are considered: V_0=5, 10 and 20 m/s. The results are presented in Fig. 10(a). We can conclude

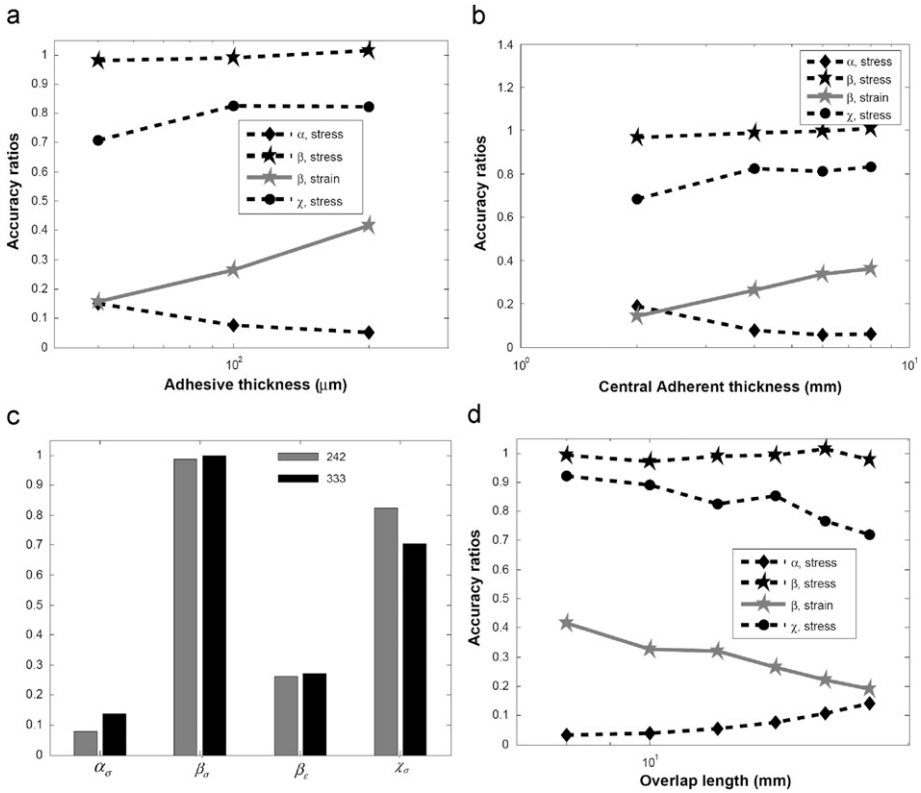

Fig. 9. Influence of geometrical parameters: (a) influence of adhesive thickness, (b) influence of adherends thicknesses, (c) comparison between '242' and '333' and (d) influence of overlap length.

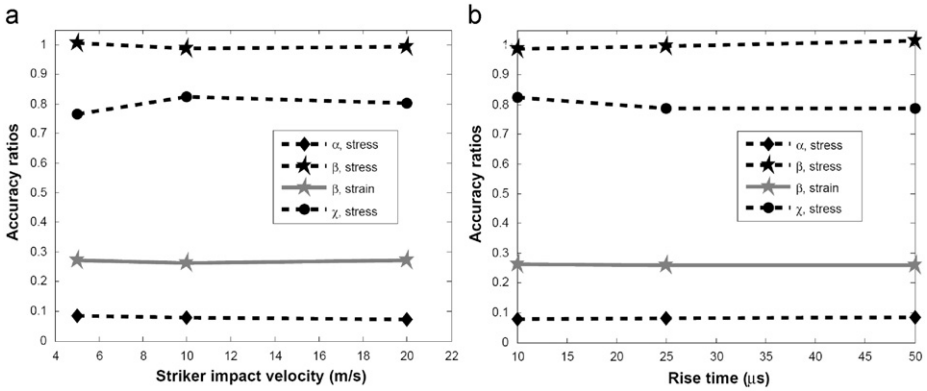

Fig. 10. Influence of dynamic parameters: (a) influence of impact velocity and (b) influence of loading rise time.

that the above studied parameters are insensitive to the striker velocity. This can be explained by the fact that the studied parameters are analysed for $t > t_h$. For these times, wave-propagation-induced heterogeneity disappears. Only, the structure-induced heterogeneity remains. We can expect that dynamic parameters have no influence at these times of the test.

3.4.2. Influence of the rise-time

It is well known in literature that pulse-shaping can help the establishment of the dynamic equilibrium [43,44]. On the other hand, the pulse shaping modifies the rise time τ_d (see Fig. 3). Adamvalli and Parameswaran [16] studied experimentally three configurations: a direct impact of the striker on the input bar (no pulse shaper) and two loading pulse shaper. In the absence of pulse shaper, the rise time was 14 μs. The used pulse shapers were 0.3 and 0.6 mm-thick annealed copper disks and yield rise times of 35 and 65 μs, respectively. In this paper, we considered three rise-time values: $\tau_d = 10$, 25 and 50 μs. It appears in Fig. 10(b) that the rise time has no influence on the studied parameters. Indeed, this parameter can influence the first part of the test, i.e., for $t < t_h$. t_h is lower than 20 μs for the considered rise times. However, once the dynamic equilibrium is established, the strain and strain heterogeneity is due only to structural effects.

4. Discussions

In this paper, we developed a numerical model for a SHPB test on adhesively bonded joint. Furthermore, we investigated the influence of geometrical, material and dynamic parameters on the accuracy of such test. Seven parameters were studied in this work. Dynamic parameters have almost no influence. It is worth to notice that the study is focused on times $t > t_h$, i.e., for the test period when the dynamic heterogeneity disappears. This is motivated by the fact that for all studied configurations, t_h is lower than 20 μs. On the other hand, the fracture occurs for brittle adhesive after 50 μs and later for the ductile ones. Therefore, the fracture occurs once the dynamic heterogeneity disappears. As the dynamic experiments on adhesive joints are usually interested in the fracture behaviour, the above defined ratios are pertinent.

The influence of adherends Young's modulus and, adhesive and adherends thicknesses have the same tendency. Furthermore, the influence of the adhesive Young's modulus is the same as that of the overlap length. Therefore, we define a unified parameter:

$$\lambda = \frac{E_1 h_0 h_1}{E_0 l_0}, \tag{18}$$

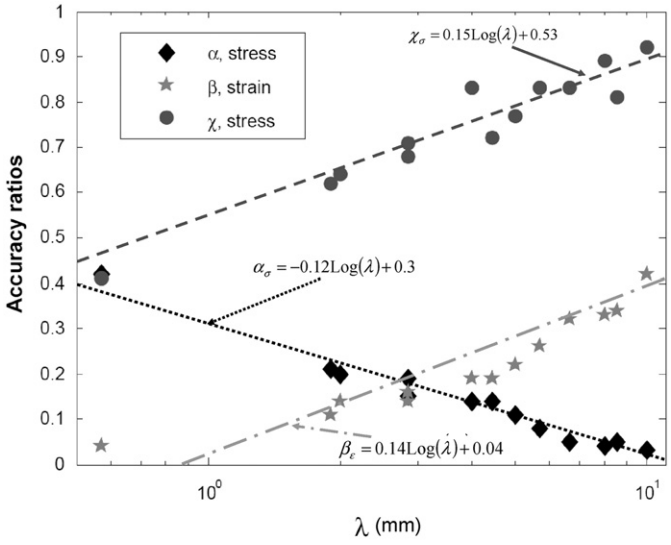

Fig. 11. Influence of the $\lambda = E_1 h_0 h_1 / E_0 l_0$ parameter.

which has the dimension of a length. Subsequently, we studied its influence on the above defined ratios. In Fig. 11, we plot the sensitivity of α_σ, χ_σ and β_ε to the logarithm of λ. The relationships are almost linear and can be approximated by the following equations:

$$\alpha_\sigma \approx -0.12\log(\lambda) + 0.3, \tag{19}$$

$$\chi_\sigma \approx 0.15\log(\lambda) + 0.53, \tag{20}$$

$$\beta_\varepsilon \approx 0.14\log(\lambda) + 0.04. \tag{21}$$

Eqs. (19) and (20) are valid for λ ranging from 0.5 to 10 mm and Eq. (21) is valid for λ between 1 and 10 mm. Furthermore, we can assume, for the same ranges of λ, that $\alpha_\varepsilon \approx \alpha_\sigma$, $\chi_\varepsilon \approx \chi_\sigma$ and $\beta_\sigma \approx 1$.

It is worth to notice, the increase of the ratio E_1/E_0 tends to increase λ and subsequently improve homogeneity and accuracy of the SHPB method. Indeed, when E_1/E_0 is high, the adhesive stiffness tends to be much lower than the adherends stiffness. In this case, the strain and stress in the adhesive are almost constant. Furthermore, the adhesive shear strain is simply expressed by adherends displacements as assumed in Eq. (10).

Eqs. (19)–(21) can be used for two applications. Firstly, they can be used to calculate the specimen geometry. Precisely, when $\lambda > 10$ mm, we can assume that the stress distribution is

homogeneous. Indeed, for this range of λ, we have $\chi_\sigma > 0.9$ and $\alpha_\sigma < 0.03$. This means that the difference between the maximum and mean stress is less than 10%. Furthermore, the stress deviation is less than 3% of the mean stress. Knowing the adhesive and adherends Young's modulii, a criterion to calculate specimen dimensions is

$$\frac{h_0 h_1}{l_0} > 10\frac{E_0}{E_1}. \tag{22}$$

Note that the used unit for h_0, h_1 and l_0 is mm.

Nevertheless, the optimal geometry design by Eq. (22) is not always possible. Furthermore, there will be always problem on the strain measurement. Indeed, $\beta_\varepsilon < 0.5$ for the considered range of λ, i.e., the mean strain in adhesive layer is less than 50% of the strain recovered by the SHPB method. In these cases, Eqs. (19)–(21) can be used as correction coefficients.

Experimentally, we can recover the stress and strain by the SHPB method, i.e., σ^{SHPB} and ε^{SHPB}, respectively. As $\beta_\sigma \approx 1$, the actual mean stress and strain in adhesive layer can be recovered by

$$\sigma^{avg} \approx \sigma^{SHPB} \tag{23}$$

and

$$\varepsilon^{avg} \approx \beta_\varepsilon \varepsilon^{SHPB}, \tag{24}$$

respectively. We recall that β_ε can be computed by Eq. (21). Similarly the maximum stress and strain in the adhesive layer can be calculated by

$$\sigma^{\max} \approx \frac{1}{\chi_\sigma}\sigma^{SHPB} \tag{25}$$

and

$$\varepsilon^{\max} \approx \frac{\beta_\varepsilon}{\chi_\varepsilon}\sigma_{SHPB}, \tag{26}$$

respectively. We recall that $\chi_\varepsilon = \chi_\sigma$ and χ_σ is given by Eq. (20).

5. Conclusions

SHPB tests, on double-lap bonded joints, were simulated using a three-dimensional finite element method. Subsequently, several ratios were defined in order to measure the accuracy of the SHPB method. Furthermore, we investigated the influence of several material, geometrical and dynamic parameters on the accuracy ratios. It was concluded that the SHPB method is accurate when recovering the mean value of the stress in the adhesive layer. Nevertheless, the conventional SHPB recovery inaccurately estimates the mean value of adhesive strain field and the maximum values of the adhesive stress and strain fields. Therefore, we defined a unified parameter, in order to help designing of the tested specimens. This parameter is the product of the adherend Young's modulus and the adhesive and adherends thicknesses divided by the product of the adhesive Young's modulus and the overlap length. We showed that the accuracy defined ratios are almost linear in terms of the logarithm of this unified parameter. This linear relationship can be used in order to correct the stress and strain recovered by the SHPB method.

Acknowledgement

The CNRS-Liban (Lebanon National Council for Scientific Research) is highly acknowledged for the financial support to the first author.

References

[1] Kinloch AL, Kodokian JA. J Adhes 1987;24:109.
[2] Perry HA. Adhesive bonding of reinforced plastics. New York: McGraw-Hill; 1959.
[3] Pang SS, Yang C, Zhao Y. Compos Eng 1995;5:1011–27.
[4] Sato C, Ikegami K. J Adhes 1999;70:57–73.
[5] Wada H, Kubo S, Murase K. J Soc Mater Sci Jpn 2001;50:223–8.
[6] Yokoyama T. J Strain Anal Eng Des 2003;38:233–45.
[7] Yokoyama T, Nakai K. J Phys IV 2006;134:789–95.
[8] Beevers A, Ellis MD. Int J Adhes Adhes 1984;4:13–6.
[9] Harris JA, Adams RD. Proc Inst Mech Eng C2 1985;199:121–31.
[10] Lataillade JL, Cayssials F. Polym Eng Sci 1997;37:1655–63.
[11] Bezemer AA, Guyt CB, Vlot A. Int J Adhes Adhes 1998;18:225–60.
[12] Keisler C, Lataillade JL. J Adhes Sci Technol 1995;9:395–411.
[13] Yokoyama T. Key Eng Mater 1998;145–149:317–22.
[14] Yokoyama T, Simizu H. JSME Int J Ser A 1998;41:503–9.
[15] Srivastava V, Shukla A, Parameswaran V. J Test Eval 2000;28:438–42.
[16] Adamvalli M, Parameswaran V. Int J Adhes Adhes 2008;28:321–7.
[17] Challita G, Othman R, Guégan P, Khalil K, Poitou A. Int J Mod Phys B 2008;22:1081–6.
[18] Goglio L, Rossetto M. Int J Impact Eng 2008;35:635–43.
[19] Lawrence Wu CM, Li RKY, Yeung NH. J Electron Packag Trans ASME 2003;125:93–7.
[20] Rao Y, Lu D, Wong CP. Int J Adhes Adhes 2004;24:449–53.
[21] Zachary LW, Burger CP. Exp Mech 1980;20:162–6.
[22] Kaya A, Tekelioglu MS, Findik F. Mater Lett 2004;58:3451–6.
[23] Adams RD, Harris JA. Int J Adhes Adhes 1996;16:61–71.
[24] Sawa T, Senou Y, Okuno H, Hagiwara H. J Adhes 1996;59:1–16.
[25] Higuchi I, Sawa T, Suga H. J Adhes Sci Technol 2002;16:1327–42.
[26] Vaidya UK, Gautam ARS, Hosur M, Dutta P. Int J Adhes Adhes 2006 184–98.
[27] Higuchi I, Sawa T, Okuno H. J Adhes 1999;59–82.
[28] Sato C, Ikegami K. Int J Adhes Adhes 2000;20:17–25.
[29] Higuchi I, Sawa T, Suga H. J Adhes Sci Technol 2002;16:1585–601.
[30] Sawa T, Higuchi I, Suga H. J Adhes Sci Technol 2003;17:2157–74.
[31] ASTM D950-03, Standard test method for impact strength of adhesive bonds. ASTM Int, 2003.
[32] ISO EN11343 Adhesives—determination of dynamic resistance to cleavage of high-strength adhesive bonds under impact conditions—wedge impact method, 1993.
[33] Othman R, Bussac MN, Collet P, Gary G. J Phys IV 2003;110:397–404.
[34] Othman R, Gary G. Exp Mech 2007;47:295–9.
[35] Othman R, Bussac MN, Collet P, Gary G. C R Acad Sci Sér 2001;329:369–76.
[36] Bussac MN, Collet P, Gary G, Othman R. J Mech Phys Solids 2002;50:321–49.
[37] Meng H, Li QM. Int J Impact Eng 2003;28:537–55.
[38] Song B, Chen W. Exp Mech 2004;44:300–12.
[39] Zhao H. Comput Struct 2003;81:1301–10.
[40] Kajberg J, Lindvist G. Int J Solids Struct 2004;41:3439–59.
[41] Kajberg J, Wikman B. Int J Solids Struct 2007;44:145–64.
[42] Aloui S, Othman R, Guégan P, Poitou A, ElBorgi S. Mech Res Commun 2008;35:392–7.
[43] Frew DJ, Forrestal MJ, Chen W. Exp Mech 2001;41:40–6.
[44] Frew DJ, Forrestal MJ, Chen W. Exp Mech 2002;42:93–106.
[45] Goland M, Reissner E. Trans ASME J Appl Mech 1944;5:A17–27.
[46] Sawa T, Suga H. J Adhes Sci Technol 1996;10:1255–71.
[47] Sawa T, Liu J, Nakano Y, Tanaka Y. J Adhes Sci Technol 2000;14:43–66.
[48] Gray III GT. ASM handbook: mechanical testing and evaluation 2000 477–87.
[49] Gary G. Techniques de l'ingénieur BM 7 176, 2000, p. 1–10.
[50] Field JE, Walley SM, Proud WG, Goldrein HT, Siviour CR. Int J Impact Eng 2004;30:725–75.
[51] Gama BA, Lopatnikov SL, Gillespie Jr JW. Appl Mech Rev 2004;57:223–50.
[52] Kolsky H. Proc Phys Soc B 1949;62:676–700.
[53] Hopkinson B. Philos Trans Roy Soc A 1914;213:437–52.
[54] Zhao H, Gary G. J Mech Phys Solids 1995;43:1335–48.
[55] Othman R, Blanc RH, Bussac MN, Collet P, Gary G. C R Mécanique 2002;320:849–55.